06;01;15

Thermal decomposition of polymethylmethacrylate and its composite with fullerene C_{60} after ultraviolet irradiation

© *A.O. Pozdnyakov*

Ioffe Institute, St. Petersburg, Russia
E-mail: ao.pozd@mail.ioffe.ru

Received September 6, 2021
Revised April 22, 2022
Accepted April 22, 2022

The analysis of the ultraviolet induced transformation of the thermal decomposition spectra of the monomer of the submicrometer layers of polymethylmethacrylate and its composite with fullerene C_{60} for different fullerene concentrations and irradiation doses has been carried out. Formation of the new decomposition stages in the spectra has been interpreted by the binding between C_{60} and side ester groups of polymethylmethacrylate.

Keywords: polymethylmethacrylate, fullerene, ultraviolet irradiation, thermal decomposition, mass–spectrometry.

DOI: 10.21883/TPL.2022.06.53787.19016

Ultraviolet (UV) irradiation is an important element of processing polymer surfaces [1,2]. The method of thermal desorption mass–spectrometry (TDMS) and its widely used analog, namely, thermal gravimetric analysis, are often used to analyze molecular mechanisms for thermal decomposition of both neat polymers and their composites [3–8], including those after irradiation. TDMS spectra of monomers of polymethylmethacrylate (PMMA) homologues can depend on the thickness of heated films [9]. It was shown for PMMA [9] that the effect of diffusion of radical reaction products on the TDMS spectrum shapes becomes negligible when their diffusion time is comparable with the time of radical coupling reactions. This condition is met at submicron film thicknesses. Previous studies [10,11] showed that when submicron films of neat PMMA and its homologue polybutylmethacrylate (PBMA) are UV–irradiated, the TDMS monomer spectrum begins exhibiting additional stage of low–temperature decomposition. Intensification of this stage is suppressed by introducing C_{60} molecules into the polymer. For PBMA, transformation of TDMS spectra of the PBMA–C_{60} composite was studied at different irradiation doses and C_{60} concentrations. In this work, a similar analysis of TDMS spectra was carried out for the first time for PMMA–C_{60} composite films.

In the study, PMMA (mean–weighted molecular weight of $5 \cdot 10^5$, Fluka), fullerene C_{60} (sublimed, 99.9%, Aldrich) and toluene ACS were used. The films were fabricated from the toluene (Tol.) solution of pure PMMA and of a mixture of separately prepared toluene solutions of fullerene and PMMA. The initial solutions and their mixtures were kept prior to using for a few days. In this paper, the films with the fullerene concentrations of ~ 2 and 8% of the composite film weight were considered. The rated compositions of two triple mixtures used in the study were as follows: $\sim 99.857\%$ Tol/0.14% PMMA/0.0028% C_{60} (2% of C_{60} in the film) and $\sim 99.859\%$ Tol/0.1293% PMMA/0.01125% C_{60} (8% of C_{60} in the film). Hereinafter, the values are given in mass percent. A rated amount of the solution ($\sim 20\,\mu$l) was cast with microsyringe Hamilton on the pre–specified area of $\sim 1\,\text{cm}^2$ of the tantalum substrate–heater (α-Ta, $\sim 99.5\%$ pure, ~ 10 cm/0.7 cm/200 μm in size, $\sim 0.05\,\mu$m in roughness). The calculated film thickness was $\sim 0.2\,\mu$m. This film thickness provides minimization of the distortions of TDMS spectra by diffusion of the decomposition products through the film [9] and UV absorption through the composite film depth. Irradiation was performed in ambient conditions by using lamp DRT-125 (effective spectral range of 230–400 nm, nominal power of 125 W, the distance between the sample surface and lamp of ~ 5 cm). TDMS spectra were detected during heating the substrate in the mode close to the heating function $T(t) = T_0 + A\exp(-t/\tau)$, where $T(t)$ is the substrate temperature, t is the time (in seconds), A andτ are parameters. Mass–spectra were detected with a reflection time–of–flight mass–spectrometer based on the MSH-6 setup (ionizing electron energy ~ 100 eV). The total pressure in the vacuum chamber of MS was measured with a cold cathode — Pirani gauge (Dual Mag 972B), the substrate temperature was measured with a chromel–alumel thermocouple welded to the side of the Ta foil opposite to that where the film studied is cast. Mass spectra, total pressure and temperature were synchronized at each time point of measurements by using digital oscilloscope DPO4034 (Tektronix) and processed with a LabView–based program code. Intensity of the methylmethacrylate (MMA) mass–spectrum line was detected by strobing the spectrum main lines $m/z = 41, 69, 100$ a.m.u. The experiments commenced after reaching the residual pressure of $\sim 10^{-7}$ Torr. To select experimental temperature regimes, preliminary analysis was perfomed over TDMS spectrum distortions related to the probable decrease in the fraction of the ions getting into the MS free drift area with increasing their amount in the ion source [12]. The analysis showed the absence of spectrum distortions at

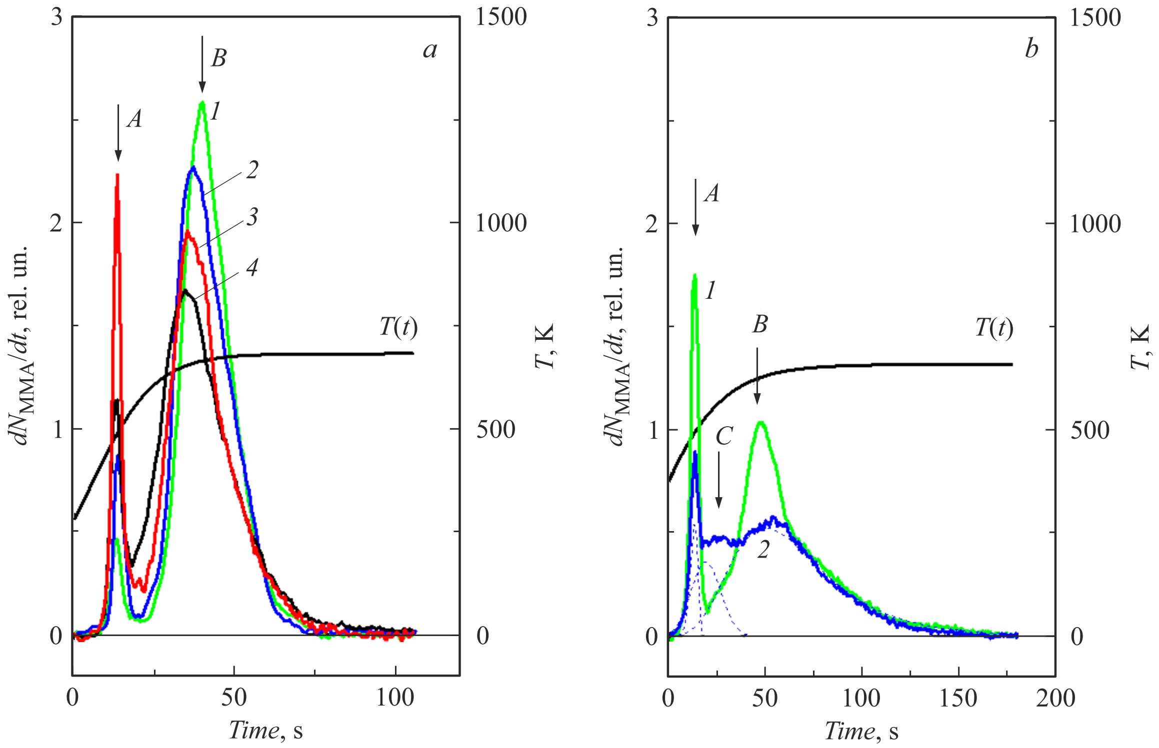

Figure 1. Time dependences of the MMA monomer desorption rate and substrate temperature $T(t)$. *a* — PMMA prior to (*1*) and after irradiation with expositions of 20 (*2*), 180 (*3*), and 2000 s (*4*). The heating function parameters are: $T_0 \sim 685$ K, $\tau \sim 16$ s. *b* — PMMA (*1*) and PMMA–C_{60} composite (*2*) after irradiation with exposition of 180 s. The C_{60} concentration in the composite is $\sim 8\%$. The dashed lines represent approximations of the composite experimental curve envelope. The heating function parameters are: $T_0 \sim 663$ K, $\tau \sim 23$ s.

pressures below $\sim 10^{-5}$ Torr. This value was not reached in the heating modes used for the studied film thicknesses. For plotting, spectra obtained in the modes of heating at the level of the thermocouple measurement error were selected. The figures present their approximation with the $T(t)$ function. In all the figures, the spectra areas were normalized to one and the same value equal to the spectrum area of pure PMMA prior to irradiation.

Prior to irradiation (Fig. 1, *a*), the pure PMMA spectra exhibit two well–resolved stages of the monomer desorption (indicated by vertical arrows *A* and *B*), at which ~ 4 and 96% of the monomer are formed, respectively. Areas of the resolved desorption stages were calculated by approximating the envelope by solutions of equations like: $dN(t)/dt = -kN(t)^m$ typical for the kinetic analysis [13]; here $k = Ae^{-U/RT(t)}$ is the rate constant (R is the gas constant, A, U, m are parameters); for this purpose, the regression analysis code [14] was used. The stage *A* relative intensity increases with increasing irradiation dose. The temperature of the stage *A* maximum increases to some extent (by ~ 10 K). At the same time, the stage *B* intensity predictably decreases. Since the number of monomers in the sample decreases with increasing irradiation dose, the curves may be corrected by the value of this decrease. However, the account of this factor is complicated by a large spread of the quantum yield of products of the PMMA side groups decomposition [15] and wide wavelength range of the UV source used in this study. After irradiating neat PMMA for ~ 180 s, the monomer fraction at stage *A* reaches $\sim 20\%$, i. e. increases by ~ 5 times with respect to that for initial PMMA. When the irradiation time exceeds ~ 180 s, relative increase in the stage *A* intensity is not detected, and stage *B* obtains more asymmetric character in the low–temperature range. For comparison, Fig. 1, *b* presents the spectra of irradiated films of neat PMMA and its composite with C_{60} in the heating regime with the limiting heating temperature $T_0 \sim 663$ K. This temperature is ~ 20 K lower than that in the heating regime used in the case illustrated by Fig. 1, *a*. Relative reduction of stage *B* in the heating regime with the lower T_0 is natural because of the reduced heating rate in the vicinity of this stage. Analysis of the curves by using the solutions of kinetic equation provides a good agreement ($\sim 2\%$) between the desorption stage areas at different heating regimes.

Fig. 2 presents the spectra of the PMMA–C_{60} composites prior to the photolysis and after the photolysis conducted during ~ 180 s. In this figure, curves *4*correspond to the pure PMMA spectrum after irradiation with the same dose. This spectrum exhibits a well–pronounced kink in stage *B*. The detection of this kink allows considering it as a superposition of two decomposition stages (the approximations are represented by dashed lines). Stage *B*

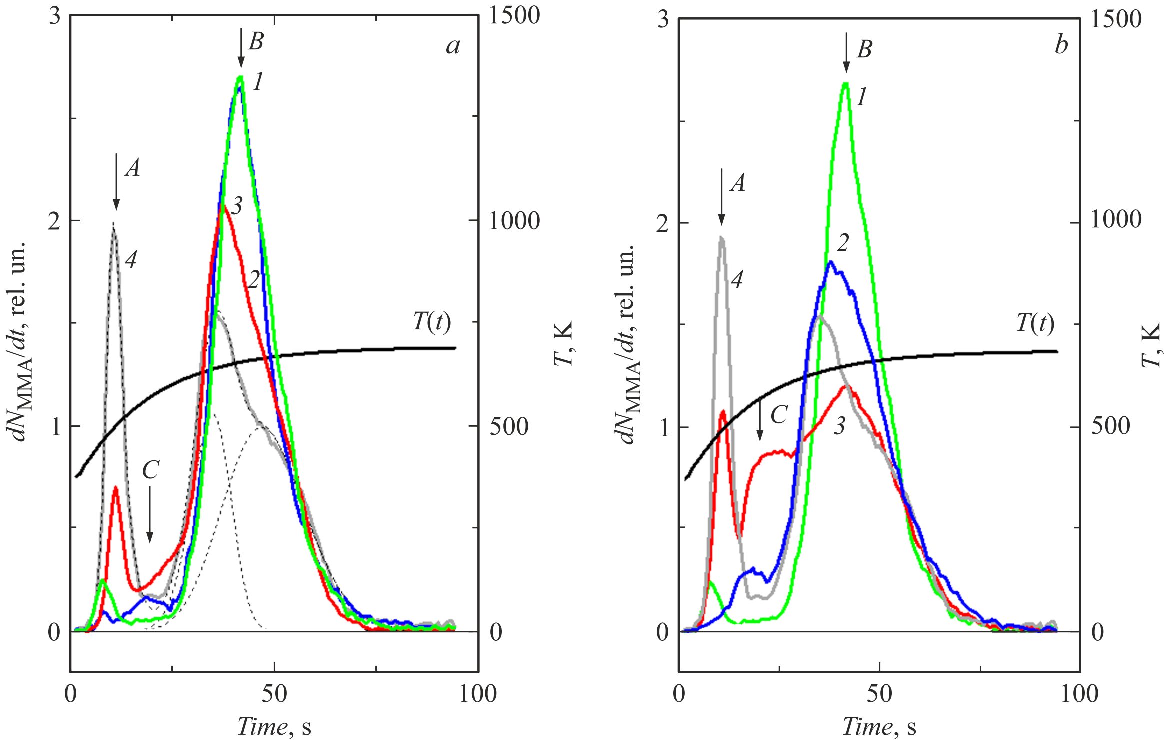

Figure 2. Time dependences of the MMA monomer desorption rate and substrate temperature $T(t)$ at the heating function parameters $T_0 \sim 690$ K, $\tau \sim 19$ s. *1* — PMMA, *2* — PMMA–C_{60} composite prior to irradiation, *3* — PMMA–C_{60} composite after irradiation with exposition of 180 s. *4* — the pure PMMA spectrum after irradiation with exposition of 180 s. Dashed lines (panel *a*) represent the stages used to approximate the pure PMMA spectrum after irradiation with exposition of 180 s (see the text).

in the spectrum of unirradiated composite with fullerene concentration ~ 2% (Fig. 2, *a*) is almost identical to that of the pure PMMA spectrum; the stage *A* intensity decreases, and a low–intensity stage *C* appears in the interval between the *A* and *B* stages. After the photolysis, the intensity of stage *A* increases (curve *3*) and reaches ~ 35% of this stage intensity in irradiated pure PMMA (curve *4*); the intensity of stage *B* decreases, while that of stage *C* slightly increases.

In the spectrum of unirradiated PMMA–C_{60} composite with the C_{60} concentration of ~ 8% (Fig. 2, *b*), the stage *C* intensity increases additionally. At the same time, the stage *B* intensity decreases, while its shape becomes more symmetric. After the photolysis, the stage *C* intensity increases even more. Along with this, the stage *B* intensity decreases below the level observed in the neat PMMA spectrum at the same irradiation dose. Since at the selected irradiation dose the neat PMMA spectrum features in the stage *C* range are less intense than those of the composite, the composite spectrum in this temperature range may be assumed to be caused by the UV–induced formation of the C_{60} covalent bonds with macromolecular side groups. The possibility of formation of these bonds is consistent with the quantum chemistry calculations [16]. The increase in the stage *C* intensity in the composite spectra prior to irradiation may evidence for that a similar binding mechanism takes place also upon heating. In the case of complete molecular dispersion of the C_{60} molecules in polymer matrix, one could expect that the increase in the fullerene concentration would decrease intensity of stage *A* at the same irradiation dose. This is not evident in visual comparison of spectra presented in Fig. 2, *a* and *b*. Tentatively, this may be explained both by overlapping of stages *A* and *B* and possible aggregation of the C_{60} molecules [17]. The latter reduces the number of effective contacts between the components. The number of C_{60} molecules in the studied composites varies from ~ 3 to 10 pieces per macromolecule, which provides a rough estimate of binding density of fullerene molecules to side groups at the selected irradiation dose. The latter amounts to ~ 1 C_{60} molecule per 500–2000 monomers. The described approach may be useful as a tool for analyzing thermal stability of specific composites after irradiation.

Variations in the shapes of TDMS spectra of PMMA–fullerene mixtures are typically interpreted as a temperature shift of maxima of the monomer desorption stages as a result of thermally induced attachment of fullerene molecules to the radicals formed upon heating [6,7]. The data obtained show that emergence of new PMMA–fullerene binding states under UV irradiation prior to heating as such does not affect the positions of the non–irradiated PMMA decomposition stages. Irradiation results in redistribution of the monomers formed in TDMS experiment to the new decomposition stages. This reduces their number registered at the stages present in TDMS spectrum prior to irradiation.

Conflict of interests

The author declares that he has no conflict of interests.

References

[1] T. Dufour, J. Hubert, N. Vandencasteele, P. Viville, R. Lazzaroni, F. Reniers, J. Phys. D: Appl. Phys., **46** (31), 315203 (2013). DOI: 10.1088/0022-3727/46/31/315203

[2] C. Wochnowski, M.A. Shams-Eldin, S. Metev, Polym. Degr. Stab., **89** (2), 252 (2005). DOI: 10.1016/j.polymdegradstab.2004.11.024

[3] Y. Pan, Z. Guo, S. Ran, Z. Fang, J. Appl. Polym. Sci., **137** (1), 47538 (2020). DOI: 10.1002/app.47538

[4] E. Mouri, M. Moriyama, Fibers Polym., **18** (12), 2261 (2017). DOI: 10.1007/s12221-017-7663-0

[5] J. Cheng, Y. Pan, J. Yao, X. Wang, F. Pan, J. Jiang, J. Loss Prev. Process Ind., **40**, 139 (2016). DOI: 10.1016/j.jlp.2015.12.017

[6] B.M. Ginzburg, Polymer Sci. A, **54** (3), 248 (2012). DOI: 10.1134/S0965545X12030029

[7] R. Katiyar, D.S. Bag, I. Nigam, Thermochim. Acta, **557**, 55 (2013). DOI: 10.1016/j.tca.2013.01.027

[8] P. Pereira, H. Gaspar, L. Fernandes, G. Bernardo, Polym. Test., **47**, 130 (2015). DOI: 10.1016/J.POLYMERTESTING.2015.09.004

[9] L.E. Manring, D.Y. Sogah, G.M. Cohen, Macromolecules, **22** (12), 2673 (1989). DOI: 10.1021/ma00202a048

[10] O.F. Pozdnyakov, E.O. Popov, A.O. Pozdnyakov, Tech. Phys. Lett., **38** (12), 1053 (2012). DOI: 10.1134/S1063785012120097.

[11] A.O. Pozdnyakov, Tech. Phys. Lett., **45** (5), 522 (2019). DOI: 10.1134/S1063785019050298.

[12] A.A. Sysoev, M.S. Chupakhin, *Vvedenie v mass-spektrometriyu* (Atomizdat, M., 1977). (in Russian)

[13] M. Ferriol, A. Gentilhomme, M. Cochez, N. Oget, J.L. Mieloszynski, Polym. Degr. Stab., **79** (2), 271 (2003). DOI: 10.1016/S0141-3910(02)00291-4

[14] http://polycert.chph.ras.ru/fitter.htm

[15] Yu.A. Mikheev, Yu.A. Ershov, Russ. J. Phys. Chem. A, **78** (5), 661 (2004).

[16] D.R. Diniakhmetova, A.K. Friesen, S.V. Kolesov, Int. J. Quantum Chem., **120** (18), e26335 (2020). DOI: 10.1002/qua.26335

[17] A.A. Bogdanov, A.O. Pozdnyakov, Tech. Phys. Lett., **42** (1), 102 (2016). DOI: 10.1134/S1063785016010181.